Published OnlineFirst April 25, 2013; DOI: 10.1158/1535-7163.MCT-12-1176-T

Chemical Therapeutics

Molecular Cancer Therapeutics

Identification and Characterization of a Small-Molecule Inhibitor of Wnt Signaling in Glioblastoma Cells

Alessandra De Robertis[1,5], Silvia Valensin[1,5], Marco Rossi[2,5], Patrizia Tunici[2,5], Margherita Verani[1,5], Antonella De Rosa[2,5], Cinzia Giordano[2,5], Maurizio Varrone[3], Arianna Nencini[3], Carmela Pratelli[3], Tiziana Benicchi[4], Annette Bakker[6], Jeffrey Hill[7], Kanda Sangthongpitag[7], Vishal Pendharkar[7], Boping Liu[7], Fui Mee Ng[7], Siew Wen Then[7], Shi Jing Tai[7], Seong-Moon Cheong[8], Xi He[8], Andrea Caricasole[5], and Massimiliano Salerno[1,5]

Abstract

Glioblastoma multiforme (GBM) is the most common and prognostically unfavorable form of brain tumor. The aggressive and highly invasive phenotype of these tumors makes them among the most anatomically damaging human cancers with a median survival of less than 1 year. Although canonical Wnt pathway activation in cancers has been historically linked to the presence of mutations involving key components of the pathway (APC, β-catenin, or Axin proteins), an increasing number of studies suggest that elevated Wnt signaling in GBM is initiated by several alternative mechanisms that are involved in different steps of the disease. Therefore, inhibition of Wnt signaling may represent a therapeutically relevant approach for GBM treatment. After the selection of a GBM cell model responsive to Wnt inhibition, we set out to develop a screening approach for the identification of compounds capable of modulating canonical Wnt signaling and associated proliferative responses in GBM cells. Here, we show that the small molecule SEN461 inhibits the canonical Wnt signaling pathway in GBM cells, with relevant effects at both molecular and phenotypic levels *in vitro* and *in vivo*. These include SEN461-induced Axin stabilization, increased β-catenin phosphorylation/degradation, and inhibition of anchorage-independent growth of human GBM cell lines and patient-derived primary tumor cells *in vitro*. Moreover, *in vivo* administration of SEN461 antagonized Wnt signaling in *Xenopus* embryos and reduced tumor growth in a GBM xenograft model. These data represent the first demonstration that small-molecule–mediated inhibition of Wnt signaling may be a potential approach for GBM therapeutics. *Mol Cancer Ther; 12(7); 1180–9. ©2013 AACR.*

Introduction

The Wnt signaling pathways, the best studied of which is the canonical (β-catenin dependent) branch, are among the most evolutionarily conserved and universally important signaling cascades in metazoans, with key roles in cellular proliferation, differentiation, development, and function (1, 2). Dysfunctional Wnt signaling has been associated with a variety of human pathologies (3) affecting different cell types and tissues, including several types of cancer, bone diseases, and diseases of the central nervous system. An increasing number of studies suggest that aberrant Wnt signaling can be initiated by several mechanisms affecting key elements of the pathway (4–11). For instance, mutations (inactivating mutations on *APC* or *Axin1* tumor suppressor genes, or activating mutations on the *β-catenin* oncogene), autocrine activation [increased expression of pathway components including Wnt ligands, Frizzled (FZD) receptors, and Dishevelled (DVL) family members] and epigenetic phenomena (e.g., promoter hypermethylation) in negative modulators of the Wnt pathway act homeostatically (e.g., *SFRPs*, *DKKs*, and *NKDs* genes). Although studied in multiple diseases, the role and importance of the Wnt signaling pathway has not been extensively described in glioblastoma multiforme (GBM). Data in recent literature supports the role of Wnt/β-catenin signaling in glioma initiation, proliferation, and invasion (12–18). The protooncogene PLAG2, amplified in GBM, imparts stem-cell properties to glioma cells by regulating Wnt signaling (12). The interaction between the transcription factor Forkhead Box M1 (FOXM1) and

Authors' Affiliations: [1]Unit of Molecular Oncology, [2]Unit of *in vivo* Pharmacology, Departments of [3]Medicinal Chemistry, [4]Biomolecular Screening, and [5]Pharmacology, and [6]Clinical Development, Siena Biotech Medicine Research Centre, Siena, Italy; [7]Experimental Therapeutics Centre, Agency for Science, Technology and Research (A*STAR), Singapore, Singapore; and [8]The F. M. Kirby Neurobiology Center, Boston Children's Hospital, Department of Neurology, Harvard Medical School, Boston, Massachusetts

Note: Supplementary data for this article are available at Molecular Cancer Therapeutics Online (http://mct.aacrjournals.org/).

A. De Robertis and S. Valensin contributed equally to this work.

Current address for A. Bakker: Children's Tumor Foundation, New York, New York.

Corresponding Author: Massimiliano Salerno, Siena Biotech Medicine Research Centre, Via del Petriccio e Belriguardo 35, 53100, Siena, Italy. Phone 39-0577-381375; Fax: 39-0577-381303; E-mail: msalerno@sienabiotech.it

doi: 10.1158/1535-7163.MCT-12-1176-T

Published OnlineFirst April 25, 2013; DOI: 10.1158/1535-7163.MCT-12-1176-T

β-catenin is a mechanism for controlling canonical Wnt signaling and is required for glioma formation (13). RNAi-mediated depletion of the scaffold protein DVL affects proliferation and promotes differentiation of GBM cells *in vitro* and *in vivo* (16). To explore further the relevance of the Wnt pathway in GBM and to provide evidence that small-molecule inhibition of Wnt signaling has therapeutic potential in this central nervous system tumor, we show that both genetic and pharmacologic Wnt inhibition results in modulation of pathway activity at both the biochemical and functional level, and in decreased proliferative capacity both *in vitro* and *in vivo*. In addition, we report the identification and initial characterization of SEN461, a novel, potent small-molecule inhibitor of canonical Wnt signaling that acts through Axin stabilization by a mechanism that is not entirely dependent on Tankyrases, and possesses strong *in vitro* and *in vivo* antitumor activity in GBM settings.

Materials and Methods

Cell lines and human GBMs

The cell lines HEK293, A172, LN229, U87MG, U251, and T98G were obtained from the American Type Culture Collection (ATCC). DBTRG-05-MG was purchased from ICLC (Genoa, Italy), and identification and authentication was done by CELL ID System (Promega). All cell lines were cultured according to the supplier's recommendations. Primary glioma cells (GBMR9, GBMR11, GBMR16, and BTR1) were obtained from patients who had undergone surgery at the IRCCS Besta Hospital (Milan, Italy), and cultured in RPMI-1640 medium supplemented with 10% FBS. Mouse Wnt3a containing conditioned media (Wnt3a-CM), and control conditioned media (CTR-CM) from mouse L cells, were harvested according to the ATCC protocol.

Plasmids, lentiviral vectors, and protein production

For the generation of TCF-Luciferase reporter, 3 copies of a 4× TCF-responsive element were cloned into the pcDNA3.1/Zeo vector (Invitrogen) after deletion of the constitutive CMV promoter and the insertion of the Firefly Luciferase ph-FL-TK (Promega). For the TA-Renilla reporter, pcDNA3.1/Hygro (Invitrogen) and ph-RL-TK (Promega) vectors, were digested with restriction enzymes Mlu1 and BamH1 and ligated by T4-Ligase to form the final construct. Human *Axin1* and *Wnt3A* were purchased from Origene as "transfection ready" plasmids. Dominant negative TCF4 cDNA was purchased from Upstate. Human *LRP6* and *Wnt1* have been cloned into pcDNA3.1/Zeo (Invitrogen) by PCR amplification of human cDNA (Clontech). β-Catenin siRNA was purchased from Ambion. Lentiviral vectors for inducible dominant negative TCF4 (rLV-EF1-tTS, rLV-EF1-rtTA, and rLV.TRE-CMV.HA-TCF4DN) were purchased from Vectalys. To generate GST fusion proteins, the PARP domain of human TNKS1 and TNKS2 (934–1166) were synthesized (GenScript) with *Eco*RI and *Sal*I sites at the 5′ and 3′ ends of the constructs to allow in-frame subcloning into the expression vector pGEX-6P-1.

Primary screening

A structurally diverse, low-molecular weight library of 16,000 compounds was screened in stable transfected DBTRG cells containing TCF-Luciferase. For single concentration testing, 6,500 cells/well, plated in 96-well plates were incubated with compounds at 10 μmol/L [0.5% diemthylsulfoxide (DMSO) v/v] 36 hours after plating. Each compound was tested in duplicate on 2 different copy cell plates. Luciferase signal was detected using Luclite Luminescence Reporter Gene Assay System 10000 (Perkin Elmer). Data were expressed as percentage of negative control (DMSO), and the activity threshold was set to 50% reduction. For IC_{50} determination, stable transfected DBTRG cells (plated at the same density used for the single concentration testing) containing TCF-Luciferase and TA-Renilla were incubated with 8-points dilutions (from 60 to 0.185 μmol/L) compound 36 hours after plating. Each compound was tested in triplicate in a single plate. Luciferase detection was done with Dual-Luciferase Reporter Assay System (Promega). For IC_{50} calculation, the data were expressed as a percentage of negative control (DMSO) for Firefly and Renilla Luciferase independently. Values were calculated using XLFit version 4.2, with a 4 parameters sigmoid model (XLFit model 205). A luciferase biochemical assay enabled the identification of compounds acting directly on the enzyme rather than true inhibitors. Quantilum recombinant Luciferase (Promega) was employed to test compounds at single concentration (10 μmol/L). Data were expressed as a percentage of negative control (DMSO).

Auto-PARsylation reactions

To assess the effect of SEN461 and XAV939 on auto-PARsylation of Tankyrases, reactions were carried out in 40 μL volumes in the presence of the compounds (concentration varying from 0.006 to 100 μmol/L, 2.5% DMSO), 20 nmol/L GST-TNKS1/2, and 250 μmol/L NAD^+ (Sigma). Reactions were incubated at room temperature for 2 hours and then quenched by adding 10 μL of 20% formic acid. Then, 100 μL of acetonitrile was added and the samples were centrifuged for 30 minutes at 3,500 rpm, 4°C. The supernatant was transferred to a new plate and subjected to the liquid chromatography/mass spectrometry (LC/MS) analysis, to detect the formation of nicotinamide (a by-product of the PARsylation reaction).

Axin ubiquitination assay

For the ubiquitination assay, DBTRG cells were pretreated with 10 μmol/L SEN461 for 4 hours and subsequently treated with 25 μmol/L of the proteasome inhibitor MG-132 (Sigma) in combination with 10 μmol/L of SEN461 overnight. Proteins were extracted with Ripa buffer (50 mmol/L Tris–HCl ph 7.4, 150 mmol/L NaCl, 1% NP40, 0.5% Na-deoxycholate, 0.1% SDS, 1 mmol/L EDTA) supplemented with 5 mmol/L N-Ethylmaleimide

Published OnlineFirst April 25, 2013; DOI: 10.1158/1535-7163.MCT-12-1176-T

(NEM), to block the activities of deubiquitinase. To immunoprecipitate Axin2, 1 mg of total lysate was incubated 2 hours at 4°C with 3 μg of specific antibody and, subsequently, the immunocomplexes were incubated with Dynabeads Protein-A-conjugated magnetic beads (Dynal) at 4°C overnight. Samples were analyzed by Western blotting with anti-multi ubiquitin (MBL) antibody.

Immunoblotting and antibodies

Total cell lysates were prepared in radioimmunoprecipitation assay buffer (RIPA; 50 mmol/L Tris–HCl ph 7.4, 150 mmol/L NaCl, 0.1% SDS, 1% NP-40, 1 mmol/L EDTA, 0.5% Na-deoxycholate) containing fresh protease (Sigma) and phosphatase (Upstate) inhibitors cocktail. Cytosolic lysates were prepared using a cell fractionation Kit (Thermo Scientific). Commercial antibodies used in this study include anti-Axin1, anti-Axin2, anti-β-catenin, anti-P-β-catenin Ser33/Ser37/Thr41, and anti-HA (Cell Signaling Technologies), anti-TNKS (Abcam), anti-tubulin (Calbiochem), anti-GAPDH (Sigma), and anti-multi ubiquitin (MBL).

Quantitative real-time PCR

RNA was extracted from cultured cells using TRIzol reagent (Gibco) followed by isopropanol-alcohol precipitation (RNeasy Plus Mini Kit, Qiagen) before quantification. Transcript levels were assessed using the Bio-Rad iQ5 (Kit iQ SYBR Green Supermix) machine, according to the manufacturer's instructions, and each experiment was repeated 3 times using independent RNAs samples. Gene expression analysis was carried out using the human housekeeping genes, *GAPDH* and *RPL13a*. Primers for the h*Axin2* were the following: forward: 5′-CAAGGGCCAGGTCACCAA-3′; reverse: 5′-CCCCCAACCCATCTTCGT-3′.

Transfections, infections, and reporter assays

Plasmids and siRNA transfections were carried out using Lipofectamine 2000 (Invitrogen) according to the manufacturer's instructions. Inducible lentiviral expression of dominant negative TCF4 was carried out following Vectalys instructions. For reporter assays, luciferase activities were measured with the Dual Luciferase Assay Kit (Promega) according to the manufacturer's instructions, 24 hours after transient transfections or lentiviral infections. In HEK293 cells Wnt pathway was activated by ectopic expression of *Wnt1* and *Wnt3A* or through addiction of Wnt3a condition medium.

Fluorescence-activated cell sorting analysis

Cell-cycle distribution after silencing (siRNA) of β-catenin was determined by measuring the amount of cellular DNA using propidium iodide staining. For G_0/G_1 synchronization, confluent cells were maintained for 24 hours in complete medium followed by 24 hours in serum-free medium. Cells were then collected by centrifugation and fixed with 50% ethanol overnight. Following fixation, cells were washed with PBS, treated with 100 μg/mL RNAse for 15 minutes, and then incubated with 50 μg/mL propidium iodide for an additional 15 minutes. DNA content was determined using a flow cytometer (FACScalibur, BD Biosciences Immunocytometry System) by measuring propidium iodide emission at 580 nm. Cell-cycle distribution was analyzed using BD CellQuest Pro software (BD Biosciences Immunocytometry System).

Soft agar assay

In the soft agar assay, a suspension of 2.5×10^3 cells per well, containing 0.36% (wt/vol) agar, was mixed with various concentrations of compounds, SiRNA, or inducible lentiviral vectors before setting. The cell layer was overlaid onto a layer of culture medium containing 0.6% (wt/vol) agar in 24-well plates. Subsequently, the plates were kept in culture (37°C and 5% CO_2) for 14 or 21 days, depending on the cell line. At the end of the incubation, colonies were stained overnight with 5 mg/mL of MTT (Sigma) and counted using the Oxford Optronix GelCount instrument.

Xenopus experiments and *in vivo* tumor growth assay

Xenopus injections were administered as previously described (19). For the glioma xenograft model, 5×10^6 DBTRG cells were injected subcutaneously into the right flank of athymic female nude mice (CD-1 nu/nu, Charles Rivers, Calco, Italy). All mice were maintained in a conventional-specific pathogen-free facility (according to the NIH guidelines). Twice a week, tumor growth and body weight were evaluated and recorded. Dimensions of the tumors were measured by a digital caliper, and tumor masses were calculated using the following formula: length (mm) × width^2 (mm) × d/2, assuming density, $d = 1\ \text{mg/mm}^3$ for tumor tissue. When measurable tumors were established in the majority of mice, animals were randomly assigned into treatment groups (10 mice/group). Animals received the compound by oral gavage at 3 dose levels and at the dose volume of 10 mL/kg. SEN461 was administered at the following doses and schedules: 30 mg/kg twice daily for 14 consecutive days, 100 mg/kg once daily for 14 consecutive days, 500 mg/kg once weekly for 2 consecutive weeks. Mice were sacrificed when the tumors reached a volume around 10% of total body weight.

Statistical analysis

Statistical analysis for soft agar, reporter, and quantitative PCR (qPCR) assays was conducted with 1-way Anova test followed by Tukey test for multiple comparisons. Auto-PARsylation data were analyzed by nonlinear regression. Significant difference of embryos developing second axis was tested with Fischer exact test, and a *t* test was conducted on proportions to assess good reproducibility of results across the independent experiments. For the glioma xenograft model, a mixed-effects ANOVA model was conducted at the end of the study on body weight and tumor mass data considering "treatment" and "time" as main effects. Statistical analysis was

Published OnlineFirst April 25, 2013; DOI: 10.1158/1535-7163.MCT-12-1176-T

carried out using GraphPad Prism and Matlab statistical software.

Compounds

IWR2 and XAV939 molecules were purchased from Asinex and Maybridge respectively.

SEN461 [6-Methoxy-3-{4-[4-(2-methoxy-acetyl)-piperazine-1-carbonyl]-cyclohexylmethyl}-1-methyl-1H-quinazoline-2,4-dione] and SEN973 [3-[4-(4-Cyclopropanecarbonyl-piperazine-1-carbonyl)-cyclohexylmethyl]-6,7-dimethoxy-1H-quinazoline-2,4-dione] were designed and synthesized at Siena Biotech. The chemical structures are reported in Fig. 1A. Synthetic details for SEN461 are reported in the patent application WO 2011/042145 (compound 66).

All compounds tested for the *in vitro* assays were dissolved in DMSO. SEN461 was formulated in 0.5% methocel for the *in vivo* studies.

Results

Effect of Wnt pathway modulation and pathway screening approach to identify small-molecule Wnt inhibitors in glioma cells

To investigate the consequences of Wnt signaling inhibition in glioblastoma, we used the DBTRG-05MG (DBTRG) cell line (20). The cell line, originally derived from a human recurrent GBM, harbors mutations in *PTEN*, *CDKN2A*, and *BRAF*, but has a wild-type *TP53* gene (Wellcome Trust Sanger Institute: http://www.sanger.ac.uk/genetics/CGP/CellLines/). No mutations involving *APC*, *Axin*, and/or *β-catenin* genes have been reported for DBTRG cells, which are considered to have an intact canonical Wnt pathway cascade (Wellcome Trust Sanger Institute Database). We characterized this cellular system for Wnt pathway activity and relevance by specific biological and biochemical tools at the molecular and phenotypic level. In the canonical pathway, Wnt signaling activity is controlled by the intracellular β-catenin level through its phosphorylation-dependent degradation. Upon stimulation by an appropriate Wnt signal, accumulating β-catenin translocates to the nucleus, where it binds TCF (T cell factor) transcription factor (also known as lymphoid enhancer-binding factor-l, LEF1), serving as a coactivator of TCF/LEF-induced transcription and leading to increased expression of Wnt target genes (21, 22). β-catenin, therefore, represents a key intracellular effector of the genomic response of the cell to an incoming Wnt signal. The phenotypic effects of transient β-catenin knockdown via an siRNA included a decrease of a Wnt target gene *cyclin D1* (Supplementary Fig. *S*1B) and a reduction in the ability of GBM cancer cells to grow in an anchorage-independent fashion (Supplementary Fig. *S*1A), and a substantial change in the cell-cycle profile with a G_0/G_1 cell-cycle arrest and an S-phase reduction (Supplementary Fig. *S*1C), showing that cell growth is Wnt/β-catenin dependent in this glioblastoma cell line. DBTRG cells, therefore, represent a suitable model for the initial identification of small-molecule modulators of Wnt signaling with relevance for GBM.

Having selected DBTRG as a GBM cell model responsive to Wnt inhibition, we set out to develop a screening approach for the identification of compounds capable of modulating canonical Wnt signaling and associated proliferative responses in GBM cells. The screening cascade to identify Wnt signaling pathway inhibitors included cellular and biochemical-based assays. A Wnt-responsive Luciferase (TCF-Luciferase (Firefly)) and a (Wnt-independent) constitutive promoter-driven Renilla Luciferase (TA-Renilla) reporter plasmid (alone and in combination) were stably transfected in DBTRG cells and constituted our primary screening assay. As an additional validation step for this readout, we employed the dominant-negative TCF4 (dnTCF4), which cannot bind to β-catenin (23, 24). As result, the output of the Luciferase-based reporter system was strongly inhibited (Supplementary Fig. *S*1D) in a concentration-dependent fashion, indicating

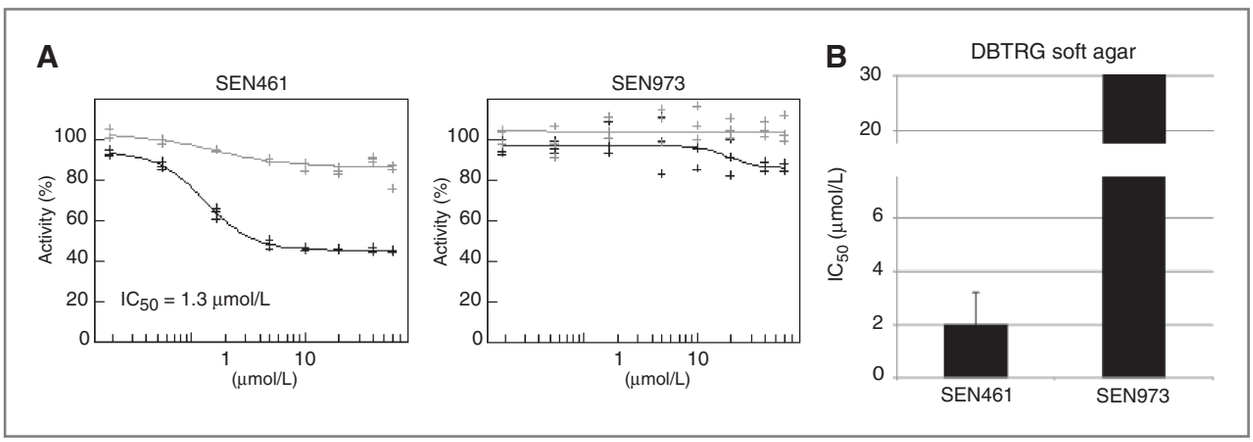

Figure 1. SEN461 inhibits Wnt-induced transcriptional activity and suppresses anchorage-independent growth of DBTRG cells. A, DBTRG cells stably transfected for TCF-Luciferase and TA-Renilla were exposed to different amounts of SEN461 or SEN973 and reporter activity was measured 24 hours later. Black and gray lines represent TCF-luciferase and TA-Renilla respectively. B, the half-maximal inhibitory concentration (IC_{50}) for DBTRG cancer cells after SEN461 and SEN973 is shown, determined from the soft agar assay.

Published OnlineFirst April 25, 2013; DOI: 10.1158/1535-7163.MCT-12-1176-T

that the reporter cell line is sensitive to genetic Wnt inhibition. A random set of 16,000 small molecules from Siena Biotech internal compounds collection was tested at single concentration (10 μmol/L) in stably transfected DBTRG-TCF-Luciferase cells. Compounds showing 50% or more inhibition were then tested in a concentration-response manner on DBTRG cells stably transfected with TCF-Luciferase and TA-Renilla plasmids in order to select the compounds displaying potency associated with minimal signs of cellular toxicity. A luciferase biochemical assay applied before hit selection enabled the identification of true inhibitors of the Wnt pathway and the elimination of compounds acting directly on the enzyme, such as luciferase modulators and/or quenchers. Several structurally distinct hit series were identified and validated. The lead compound SEN461 inhibited Wnt reporter activity in the DBTRG cell line (Fig. 1A) with an IC_{50} of 1.3 μmol/L, and affected their ability to grow in an anchorage-independent fashion (Fig. 1B); no effect either in the reporter (Fig. 1A) or in the growth-inhibition assay (Fig. 1B) was shown by SEN973 (Fig. 2), a structural analogue of SEN461 (Fig. 2).

SEN461 increases Axin and decreases β-catenin levels in DBTRG cells

In order to link inhibition of Wnt signaling and anchorage-independent growth in glioblastoma cells, we started to analyze the effect of SEN461 treatment on key components of the canonical Wnt pathway at the protein level. The effect of SEN461 on Axin steady-state protein levels was compared with that of XAV939 and IWR2 molecules (Fig. 2), 2 previously published Axin stabilizers (25, 26). DBTRG cells treated overnight with 2 different concentrations (3 and 10 μmol/L) of SEN461 showed an increase of phosphorylated β-catenin (a prerequisite for proteasome-mediated degradation of β-catenin) in the cytoplasmic fraction, which correlated with a concomitant decrease in the total amount of β-catenin, and a simultaneous accumulation of Axin1 and Axin2 compared with vehicle (DMSO)-treated cells (Fig. 3A). By contrast, the inactive structural analogue SEN973 did not produce any such effects (data not shown). As presented in Fig. 3B, all 3 small molecules showed comparable effects on the accumulation of both Axin1 and Axin2 in DBTRG cells. The increase in Axin protein levels after compound treatment could be explained by protein stabilization as reported for these recently identified inhibitors of the Tankyrase (25–27), which acts through Axin destabilization. It can be hypothesized that SEN461 treatment protected Axin from proteosomal degradation, because cotreatment of SEN461 and the reversible proteasome inhibitor MG-132 almost completely blocked the ubiquitination of Axin2 (Fig. 3C). Tankyrases, TNKS1, and TNKS2, are enzymes of the PARP family mediating the PARsylation of substrate proteins, a fundamental step in ubiquitin-mediated protein degradation. To test whether the negative modulation of Wnt activity induced by SEN461 was the consequence of the inhibition of the PARP catalytic activity of TNKS, we conducted biochemical assays for TNKS1 and TNKS2. As shown in the Supplementary Fig. *S*2A, SEN461 showed much weaker activity than XAV939 (from 300- to almost 2,000-folds) in auto-PARsylation of TNKS1 and TNKS2 (IC_{50} of 18 and 2.9 μmol/L respectively). Moreover, we also tested whether SEN461 was able to stabilize TNKS1 and TNKS2 protein levels as shown for XAV939 and IWR2 (26). There was no sign of TNKS stabilization after SEN461 treatment in DBTRG cells (regardless of the accumulation of Axin1), while both IWR2 and XAV939 induced significant TNKS stabilization (Fig. 3D), as previously reported (26). A weak TNKS stabilization was observable only following very high (100 μmol/L) exposure to SEN461 (Supplementary Fig. *S*2B). These results suggest that Axin stabilization induced by SEN461 is accompanied by minimal TNKS stabilization, implying that Axin stabilization by SEN461 occurs via a mechanism distinct from that by known TNKS inhibitors. The identification of SEN461 as a structurally novel small-molecule inhibitor of the Wnt pathway acting at the level of Axin stabilization further supports the modulation of Axin levels as a pharmacologic approach in Wnt inhibition. The comparable activity of SEN461, IWR2, and XAV939 in inhibition of TCF-Luciferase activity and GBM cell growth *in vitro* (Supplementary Fig. *S*3) suggests the relevance of such approach for the development of GBM therapeutics.

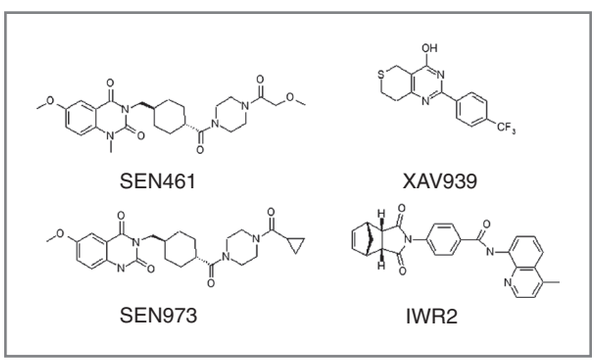

Figure 2. Chemical structures. Chemical structures of different Axin stabilizers and SEN973, an inactive structural analogue of SEN461.

In vitro and *in vivo* characterization of Wnt signaling inhibition by SEN461

To further characterize the effects of SEN461 on canonical Wnt signaling in a different, non-GBM cellular background, we investigated the compound in a nontumorigenic, immortalized cell line widely employed for Wnt studies, namely HEK293 cells, where individual Wnt ligands can be efficiently expressed and the downstream responses studied (28, 29). In order to study the effects of SEN461 on pathway stimulation by selected Wnts, we transiently cotransfected the Luciferase- and Renilla-based reporter plasmids (already employed in the screening campaign) in HEK293 cells transiently overexpressing the canonical Wnt pathway ligands *Wnt1* (Fig. 4A) or *Wnt3A* (Fig. 4B) alone or in combination with the

Published OnlineFirst April 25, 2013; DOI: 10.1158/1535-7163.MCT-12-1176-T

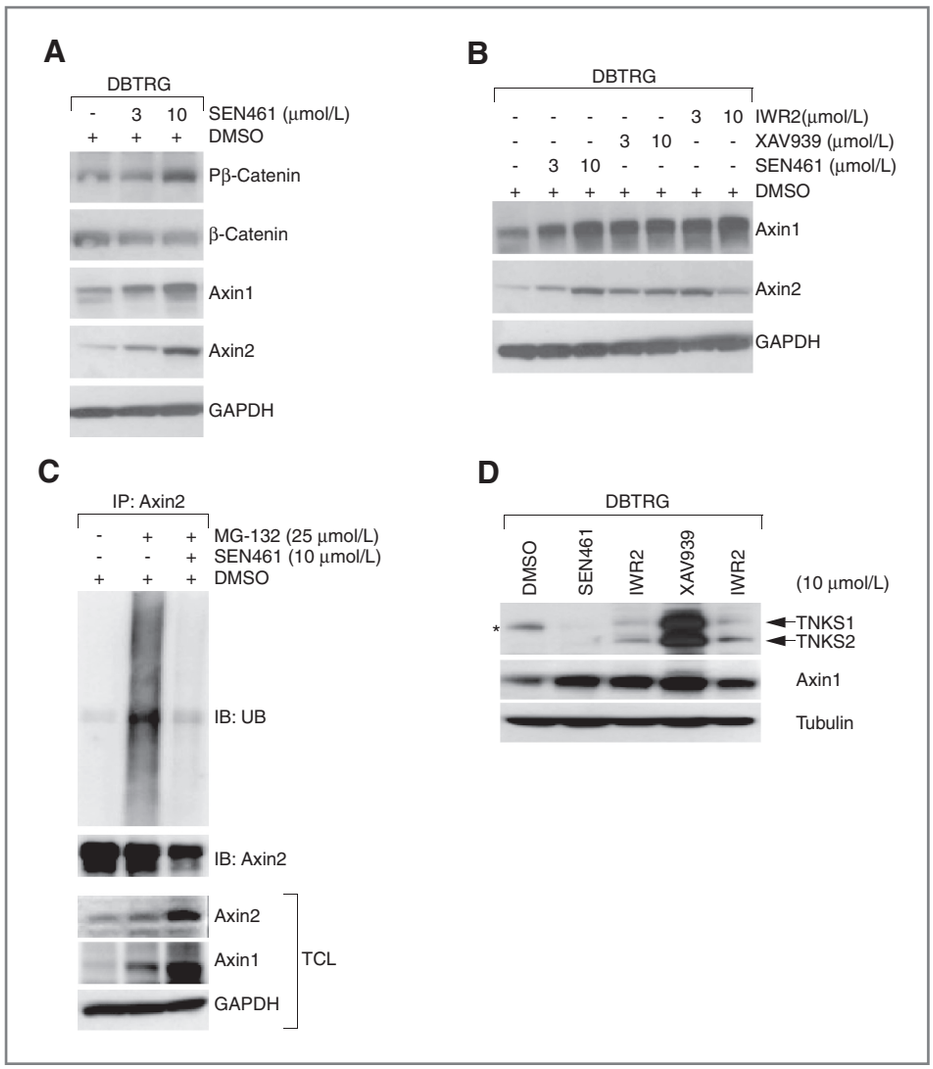

Figure 3. Effects of different compound Axin stabilizers on key protein components of the Wnt pathway in DBTRG cells. A, Western blotting analysis from cytoplasmic DBTRG lysates showing that SEN461 treatment stabilizes Axin1 and Axin2, and increases phosphorylated β-catenin (Ser33/Ser37/Thr41) with a concomitant decrease of total β-catenin. GAPDH was used as loading control. B, Western blotting from cytoplasmic DBTRG lysates after treatment with 2 different amounts of SEN461, XAV939, and IWR2 molecules showed comparable stabilization of Axin1 and Axin2 proteins. C, DBTRG cells were exposed overnight with 25 μmol/L of the proteasome inhibitor MG-132 alone or in combination with 10 μmol/L of SEN461. Lysates were immunoprecipitated with anti-Axin2 and immunoblotted with anti-ubiquitin. Total cell lysate (TCL) was analyzed by Western blotting with anti-Axin1, anti-Axin2, and anti-GAPDH. D, DBTRG cells were treated overnight with 10 μmol/L of different Wnt inhibitor molecules. Lysates were then analyzed by Western blotting with anti-TNKS (26), anti-Axin1, and anti-tubulin as loading control. The asterisk represents a background band, clearly evident in the DMSO lane, migrating below the TNKS1 band.

coreceptor *LRP6* (Supplementary Fig. S4). *Wnt1* and *Wnt3A* were selected because they represent the members of the Wnt family with the strongest association with stimulation of the canonical pathway, and because of their relevance to tumor biology (30–33). The results indicated that SEN461 inhibited with comparable potency either *Wnt1*- or *Wnt3A*-mediated luciferase activity in a concentration-dependent manner, without affecting Wnt-independent, constitutive TA-Renilla activity. Stimulation of HEK293 cells with Wnt3a exogenously provided in conditioned medium (CM) produced an increase in the amount of total β-catenin protein levels as expected after Wnt3a stimulation. SEN461 reversed the effects of Wnt3a by inducing a reduction of total β-catenin and an increment in the phosphorylated β-catenin fraction (Fig. 4C), showing that the Wnt inhibitory effect of SEN461 is not mediated through inhibition of ligand expression/secretion (as recently reported for a Porcupine inhibitor; ref. 25). Consistent with the reporter data, the mRNA levels for the Wnt/β-catenin target gene Axin2, induced by Wnt3a CM stimulation, was inhibited by SEN461 treatment (Fig. 4D). The *Xenopus* axis-duplication assay represents a valuable and sensitive way to test the *in vivo* efficacy and specificity of Wnt signaling modulators (34). Injecton of 10 pg of XWnt8 mRNA into the ventral regions of a 4-cell stage *Xenopus* embryo produced ectopic axis formation in almost 80% of the injected embryos (Fig. 5A). In contrast, coinjection of XWnt8 mRNA with 1 pmol SEN461 produced a 56% reduction of axis duplication compared with DMSO-treated embryos (Fig. 5A). These results support the specific and selective Wnt canonical inhibitory activity in both cellular-based assays and *in vivo*.

In vitro antitumor activity of SEN461 in glioblastoma cell lines

To explore the pharmacologic effects of Wnt signaling inhibition on glioblastoma cell viability, and to extend the observations obtained in DBTRG cells, we examined the

Published OnlineFirst April 25, 2013; DOI: 10.1158/1535-7163.MCT-12-1176-T

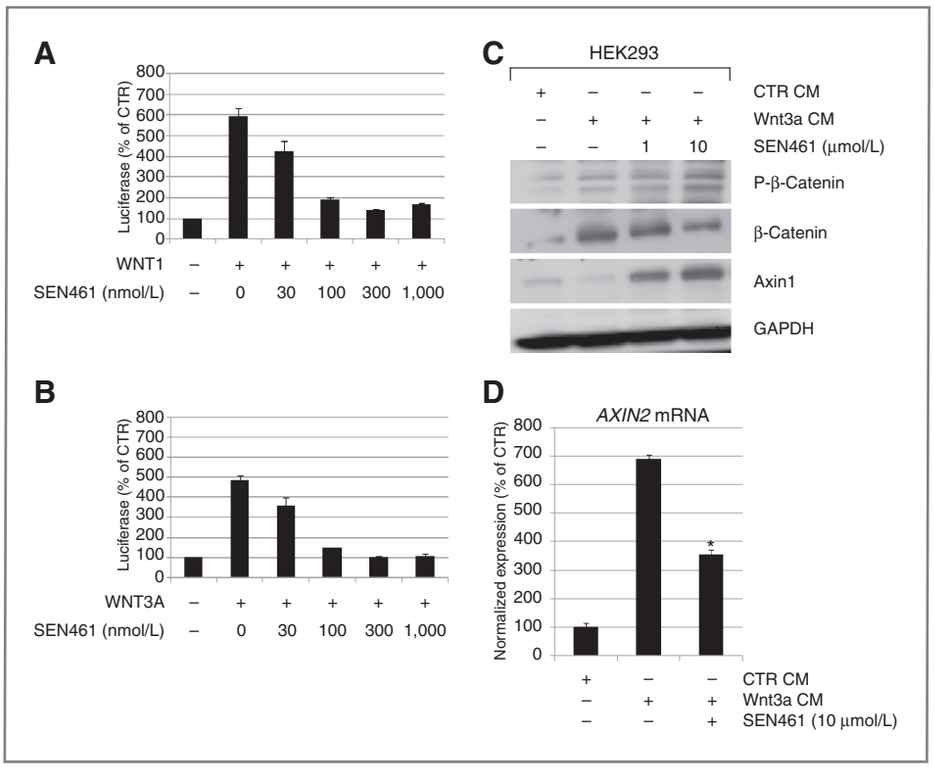

Figure 4. SEN461 affects canonical Wnt ligand-mediated transcription and modulates molecular markers of the pathway. HEK293 cells, transiently transfected with TCF-luciferase and TA-Renilla and different combinations of *Wnt1* (A) and *Wnt3A* (B) expression plasmids were either treated with DMSO (vehicle) or different amounts of SEN461. The data showed potent concentration-dependent inhibition of Wnt transcriptional activity either in Wnt1- or Wnt3A-mediated luciferase activity, without affecting Wnt-independent TA-Renilla activity. Data represent means ± SEMs. C, HEK293 cells were stimulated overnight with Wnt3a conditioned medium or control conditioned medium, alone or in combination with SEN461. Lysates were analyzed by Western blotting with total and phosphorylated anti-β-catenin and anti-Axin1. D, the effect of SEN461 treatment after Wnt3a CM stimulation on the Wnt target gene *Axin2* (mRNA) was measured by quantitative RT-PCR. Data represent means ± SEM. *, $P < 0.001$ relative to Wnt3a-stimulated cells (Tukey multiple comparison test).

consequences of SEN461 treatment in a set of 9 additional glioma cell lines, either commercially available or primary tumor, patient derived. As shown in Fig. 6A, soft agar assay results showed a wide range of sensitivities, from an IC_{50} of 0.5 μmol/L in sensitive T98G cells to more than 20 μmol/L in some cell lines. Overall, SEN461 showed significant *in vitro* activity across the panel of GBM cells tested, with most of the lines (7 out of 10) showing IC_{50} in the low micromolar range (from 0.5 to 3.5 μmol/L). To provide additional evidence that the Wnt signaling

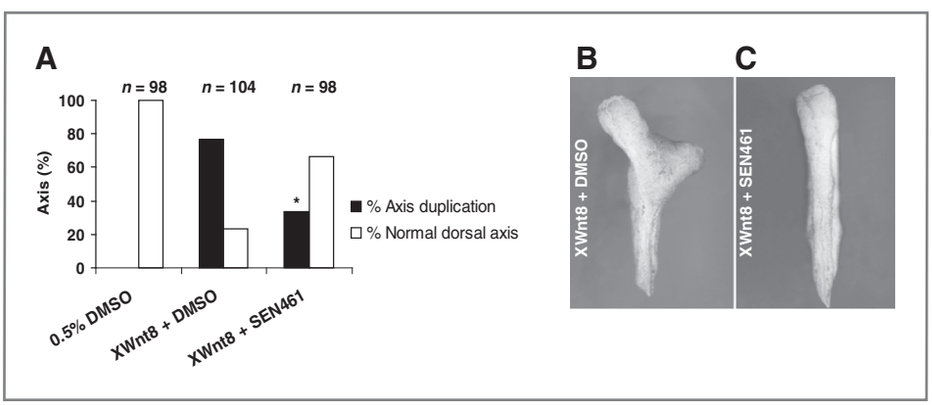

Figure 5. SEN461 inhibits XWnt8-induced axis duplication in *Xenopus* embryos. Injection of 10 pg of XWnt8 mRNA-induced axis duplication, which was inhibited by coinjection of SEN461 (1 pmol/embryo). The histogram (A) shows the percentage of embryos with normal (white bars) or duplicated axes (black bars); *n*, number of embryos examined for each group. Data collected from 3 independent experiments showed that SEN461 significantly decreased the proportion of embryos with duplicated axes (*, $P < 0.001$). Representative images of embryos with duplicated axis (B) and normal development after SEN461 coinjection (C) are shown.

Published OnlineFirst April 25, 2013; DOI: 10.1158/1535-7163.MCT-12-1176-T

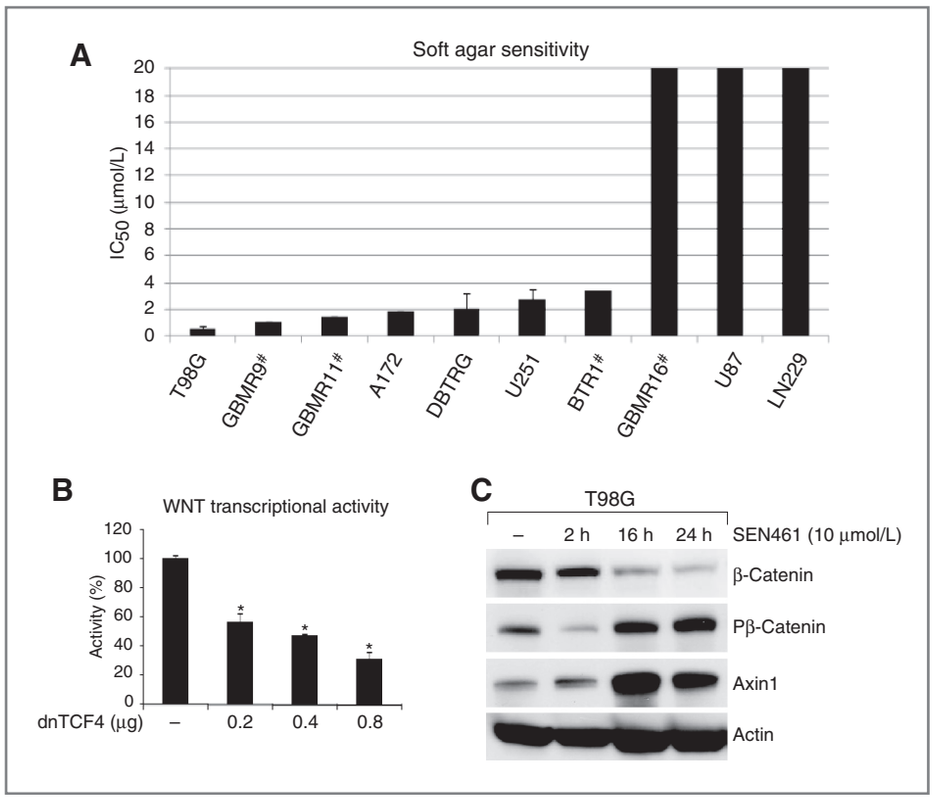

Figure 6. The response of a panel of glioblastoma cells to SEN461 *in vitro*. A, the half-maximal inhibitory concentration (IC_{50}) for 10 GBM cancer cells is shown, determined from the soft agar assay, and ranked from lowest to highest (#, primary patient-derived GBMs). B, inhibition of canonical Wnt signaling by transient transfection with dnTCF4 produced a strong concentration-dependent reduction in the Wnt transcriptional activity. Data represent means ± SEM. *, $P < 0.001$ relative to control cells (Tukey multiple comparison test). C, lysates from cells treated with SEN461 for different durations were analyzed by Western blotting with anti-P-β-catenin, anti-total-β-catenin, and anti Axin1.

activity was indeed responsible for growth inhibition, we transduced the T98G (sensitive to genetic Wnt inhibition as shown in Fig. 6B) glioblastoma cell line with a doxycycline (Doxy)-inducible dominant negative TCF4 (dnTCF4) lentivirus. As a consequence, we observed a strong decrease in anchorage-independent growth ability (Supplementary Fig. *S*5A). We next examined the effect of SEN461 treatment on β-catenin and Axin protein levels in T98G cells (Fig. 6C), where we observed a pattern resembling the one already obtained in DBTRG cells: increased phosphorylation of β-catenin and stabilized Axin1 levels, with a concomitant decrease in the cytoplasmic fraction of total β-catenin. We then asked whether overexpression of Axin1 would affect the phenotypic behaviour of the GBM cell lines examined. Indeed this was the case; Axin1 overexpression showed a profound effect on T98G (Supplementary Fig. *S*5B) as well as on DBTRG (Supplementary Fig. *S*1E) anchorage-independent growth ability, phenocopying the pharmacologic effects of SEN461 at a morphologic and molecular level.

SEN461 affects tumor growth of DBTRG xenograft model

In order to investigate the relevance of SEN461 antiproliferative capacity in an *in vivo* setting, a subcutaneous xenograft model was used to confirm the *in vitro* observation that the Wnt/β-catenin signaling pathway inhibition by SEN461 has an effect on tumor growth. Due to the very poor blood–brain barrier (BBB) penetration index of the compound (data not shown), a subcutaneous model was used instead of an orthotopic one. DBTRG cells were subcutaneously injected into CD-1 nude mice on day 0, and dosing was initiated when tumors reached a mean tumor volume of 200 mm^3. SEN461 was administered orally using 3 different schedules: 30 mg/kg twice daily (BID) for 14 consecutive days (from day 28 to 41), 100 mg/kg daily for 14 consecutive days (from day 28 to 41), and 500 mg/kg once weekly for 2 consecutive weeks (on days 28 and 34). Figure 7 shows the effect of SEN461 on tumor-volume inhibition over time until day 79 (more than a month beyond treatment and 51 days after the start of treatment). All schedules were well tolerated with no observable gross toxicities and minimal difference in body weights (Supplementary Fig. *S*6) between control- and SEN461-treated animals. Analysis on tumor mass showed a very significant effect on treatment ($P << 0.01$), and additional pair-wise comparison between treatment groups showed all treatments to be significantly different from vehicle. Significant treatment × day effect ($P << 0.01$) was observed due to a treatment-specific increase of tumor mass over time: vehicle group tumor mass significantly increased starting from day 58 with respect to day 28; on the contrary, tumor mass regrowth on SEN461 treatment is observed only after day 69. At the end of the study, all SEN461 treatments were found to be significantly different from vehicle. The antitumor activity observed for SEN461 at 30 mg/Kg BID shows the highest efficacy level (54% tumor growth inhibition with respect

Published OnlineFirst April 25, 2013; DOI: 10.1158/1535-7163.MCT-12-1176-T

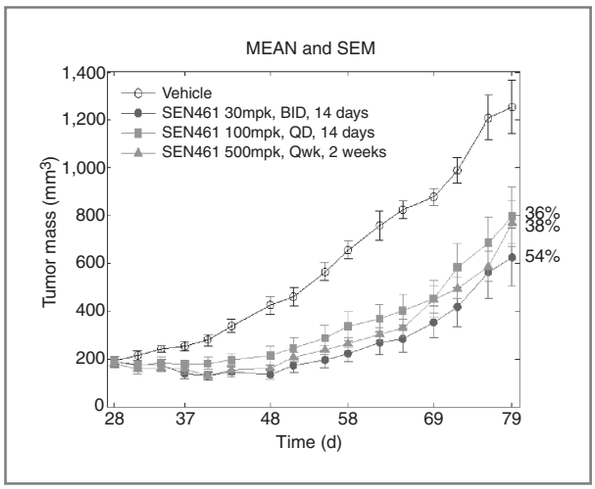

Figure 7. Antitumor activity of SEN461 in a DBTRG xenograft tumor model *in vivo*. DBTRG cells were injected s.c. into CD-1 nude mice on day 0 and SEN461 p.o. dosing started on day 28. Treatment groups (10 mice per group) received 30 mg/kg twice a day from day 28 to 41, 100 mg/kg/day daily from day 28 to 41, and 500 mg/kg/day once weekly on day 28 and 34. Tumor volume was followed over time until day 79 (37 days after the end of the treatment).

to control group) at the final endpoint (37 days after the end of the treatment).

Discussion

Despite the efforts to characterize, at the molecular level, targets and pathways that drive glioma tumorigenesis, the prognosis for patients with such brain tumors remains poor (35). The complexity of the tumor is increased by its extreme heterogeneity, supported by a vast array of genetic changes and cross-talk between signaling pathways (36, 37), which supply and sustain its high proliferation rate and its ability to infiltrate the surrounding normal parenchyma, representing the major driving force behind tumor recurrence. It has recently been reported that aberrant Wnt signaling represents a critical mechanism for the genesis, proliferation, and invasion of glioma (12–14), suggesting that inhibition of Wnt signaling provides an important approach to cancer therapies. Our data support and reinforce the involvement of the Wnt signaling pathway in glioblastoma, using either commercially available cell lines or primary patient-derived tumors. Here, we show for the first time that Wnt pharmacologic modulation in glioblastoma, mediated by a small molecule, can affect therapeutically relevant phenotypes. We show that the Wnt inhibitory compound SEN461 selectively affects canonical Wnt signaling, negatively regulates Wnt transcriptional activity in glioblastoma cell lines, inhibits XWnt8-mediated axis duplication in *Xenopus* embryos, and attenuates *in vitro* growth and *in vivo* tumorigenicity of GBM cells. The pharmacologic inhibition of the Wnt pathway by SEN461 is likely to be mediated through stabilization of Axin, which is a key negative modulator of the pathway and represents a concentration-limiting component of the β-catenin destruction complex. As a consequence, the pool of β-catenin (the phosphorylated fraction) committed to degradation increases. A critical negative role of Axin in GBM proliferation was also confirmed in DBTRG and T98G cells, where its overexpression phenocopies the pharmacologic activity of SEN461. In recent years, multiple reports (either based on mechanistic studies or pharmacologic tools) fueled interest around Axin as a potential pharmacologic target. Axin levels were, in fact, reported to inversely correlate with the grades of human astrocytoma, and its overexpression in astrocytoma cells induced cell death and reduced cell proliferation (38). The precise mechanisms regulating the degradation of Axin are, at the moment however, only partially understood, and its PARsylation by Tankyrase, its sumoylation, and its stability regulated by the ubiquitin-specific protease USP34 or by Smurf2 have recently been shown to control its ubiquitin-dependent degradation (26, 39, 40, 41). As an additional selectivity step, SEN461 activity was also biochemically tested against a panel of 48 kinases (ExpresS Diversity Kinase Profile, Cerep), where it did not show any significant activity (data not shown). Based on chemical structure diversity and biochemical and biological activity data, TNKS may not be the primary and/or direct pharmacologic target of SEN461, which we are trying to identify. In conclusion, the data presented here support the Wnt canonical signaling as a valid therapeutic opportunity to treat glioblastoma.

Disclosure of Potential Conflicts of Interest

No potential conflicts of interest were disclosed

Authors' Contributions

Conception and design: A. De Robertis, S. Valensin, A. Nencini, A. Bakker, A. Caricasole, M. Salerno, M. Varrone
Development of methodology: A. De Robertis, S. Valensin, M. Rossi, M. Verani, A. De Rosa, J. Hill, K. Sangthongpitag, L. Boping, N. Fui Mee, T-S. Wen, T-S. Jing, M. Salerno
Acquisition of data (provided animals, acquired and managed patients, provided facilities, etc.): A. De Robertis, S. Valensin, M. Verani, A. De Rosa, C. Giordano, C. Pratelli, T. Benicchi, A. Bakker, J. Hill, K. Sangthongpitag, V. Pendharkar, L. Boping, N. Fui Mee, T-S. Wen, T-S. Jing, S-M. Cheong, M. Salerno
Analysis and interpretation of data (e.g., statistical analysis, biostatistics, computational analysis): A. De Rosa, M. Varrone, T. Benicchi, A. Bakker, J. Hill, K. Sangthongpitag, V. Pendharkar, N. Fui Mee, T-S. Wen, S-M. Cheong, X. He, M. Salerno
Writing, review, and/or revision of the manuscript: A. De Robertis, S. Valensin, A. De Rosa, K. Sangthongpitag, N. Fui Mee, T-S. Wen, X. He, A. Caricasole, M. Salerno
Administrative, technical, or material support (i.e., reporting or organizing data, constructing databases): A. Nencini, T. Benicchi, K. Sangthongpitag
Study supervision: A. Bakker, M. Salerno
Other: Designed and conducted *in vivo* experiments, P. Tunici

Acknowledgments

The authors thank Letizia Magnoni and Elisa Mori for statistical support and Giuseppe Pollio and Daniela Diamanti for assistance with the reporter plasmids.

Grant Support

M. Salerno received financial support from the Monte Dei Paschi Foundation. S-M. Cheong was supported, in part, by the National

Published OnlineFirst April 25, 2013; DOI: 10.1158/1535-7163.MCT-12-1176-T

Research Foundation of Korea (NFR-2012R1A6A3A03039818). X. He was financially supported by the NIH (grant no. RO1 GM074241) and Boston Children's Hospital Intellectual and Developmental Disabilities Research Center (P30 HD-18655).

The costs of publication of this article were defrayed in part by the payment of page charges. This article must therefore be hereby marked *advertisement* in accordance with 18 U.S.C. Section 1734 solely to indicate this fact.

Received December 6, 2012; revised April 16, 2013; accepted April 16, 2013; published OnlineFirst April 25, 2013.

References

1. Nusse R, Varmus HE. Wnt genes. Cell 1992;69:1073–87.
2. Nusse R. Wnt signaling in disease and in development. Cell Res 2005;15:28–32.
3. MacDonald BT, Tamai K, He X. Wnt/beta-catenin signaling: components, mechanisms, and diseases. Dev Cell 2009;17:9–26.
4. Barker N, Clevers H. Mining the Wnt pathway for cancer therapeutics. Nat Rev Drug Discov 2006;5:997–1014.
5. Morin PJ, Sparks AB, Korinek V, Barker N, Clevers H, Vogelstein B, et al. Activation of beta-catenin–Tcf signaling in colon cancer by mutations in beta-catenin or APC. Science 1997;275:1787–90.
6. Satoh S, Daigo Y, Furukawa Y, Kato T, Miwa N, Nishiwaki T, et al. AXIN1 mutations in hepatocellular carcinomas, and growth suppression in cancer cells by virus-mediated transfer of AXIN1. Nat Genet 2000;24:245–50.
7. Benhaj K, Akcali KC, Ozturk M. Redundant expression of canonical Wnt ligands in human breast cancer cell lines. Oncol Rep 2006;15:701–7.
8. Yang L, Wu X, Wang Y, Zhang K, Wu J, Yuan YC, et al. Fzd7 has a critical role in cell proliferation in triple negative breast cancer. Oncogene 2011;30:4437–46.
9. Uematsu K, He B, You L, Xu Z, McCormick F, Jablons DM. Activation of the Wnt pathway in non small cell lung cancer: evidence of dishevelled overexpression. Oncogene 2003;22:7218–21.
10. Bafico A, Liu G, Goldin L, Harris V, Aaronson SA. An autocrine mechanism for constitutive Wnt pathway activation in human cancer cells. Cancer Cell 2004;6:497–506.
11. Rajan N, Burn J, Langtry J, Sieber-Blum M, Lord CJ, Ashworth A. Transition from cylindroma to spiradenoma in CYLD-defective tumours is associated with reduced DKK2 expression. J Pathol 2011;224:309–21.
12. Zheng H, Ying H, Wiedemeyer R, Yan H, Quayle SN, Ivanova EV, et al. PLAGL2 regulates Wnt signaling to impede differentiation in neural stem cells and gliomas. Cancer Cell 2010;17:497–509.
13. Zhang N, Wei P, Gong A, Chiu WT, Lee HT, Colman H, et al. FoxM1 promotes β-catenin nuclear localization and controls Wnt target-gene expression and glioma tumorigenesis. Cancer Cell 2011;20:427–42.
14. Augustin I, Goidts V, Bongers A, Kerr G, Vollert G, Radlwimmer B , et al. The Wnt secretion protein Evi/Gpr177 promotes glioma tumourigenesis. EMBO Mol Med 2011;4:38–51.
15. Pu P, Zhang Z, Kang C, Jiang R, Jia Z, Wang G, et al. Downregulation of Wnt2 and beta-catenin by siRNA suppresses malignant glioma cell growth. Cancer Gene Ther 2009;16:351–61.
16. Pulvirenti T, Van Der Heijden M, Droms LA, Huse JT, Tabar V, Hall A. Dishevelled 2 signaling promotes self-renewal and tumorigenicity in human gliomas. Cancer Res 2011;71:7280–90.
17. Lambiv WL, Vassallo I, Delorenzi M, Shay T, Diserens AC, Misra A, et al. The Wnt inhibitory factor 1 (WIF1) is targeted in glioblastoma and has a tumor suppressing function potentially by induction of senescence. Neuro Oncol 2011;13:736–47.
18. Jin X, Jeon HY, Joo KM, Kim JK, Jin J, Kim SH, et al. Frizzled 4 regulates stemness and invasiveness of migrating glioma cells established by serial intracranial transplantation. Cancer Res 2011;71:3066–75.
19. Semënov MV, Tamai K, Brott BK, Kühl M, Sokol S, He X. Head inducer Dickkopf-1 is a ligand for Wnt coreceptor LRP6. Curr Biol 2001;11:951–61.
20. Kruse CA, Mitchell DH, Kleinschmidt-DeMasters BK, Franklin WA, Morse HG, Spector EB, et al. Characterization of a continuous human glioma cell line DBTRG-05MG: growth kinetics, karyotype, receptor expression, and tumor suppressor gene analyses. *In Vivo* Cell Dev Biol 1992;28A:609–14.
21. Clevers H. Wnt beta-catenin/signaling in development and disease. Cell 2006;127:469–80.
22. Moon RT, Kohn AD, De Ferrari GV, Kaykas A. Wnt and β-catenin signaling: diseases and therapies. Nat Rev Genet 2004;5:691–701.
23. Van De Wetering M, Sancho E, Verweij C, de Lau W, Oving I, Hurlstone A, et al. The beta-catenin/TCF-4 complex imposes a crypt progenitor phenotype on colorectal cancer cells. Cell 2002;111:241–50.
24. Kolligs FT, Nieman MT, Winer I, Hu G, Van Mater D, Feng Y, et al. ITF-2, a downstream target of the Wnt/TCF pathway, is activated in human cancers with β-catenin defects and promotes neoplastic transformation. Cancer Cell 2002;1:145–55.
25. Chen B, Dodge ME, Tang W, Lu J, Ma Z, Fan CW, et al. Small molecule–mediated disruption of Wnt-dependent signaling in tissue regeneration and cancer. Nat Chem Biol 2009;5:100–7.
26. Huang A, Mishina YM, Liu S, Cheung A, Stegmeier F, Michaud GA, et al. Tankyrase inhibition stabilizes axin and antagonizes Wnt signaling. Nature 2009;461:614–20.
27. Waaler J, Machon O, Tumova L, Dinh H, Korinek V, Wilson SR, et al. A novel tankyrase inhibitor decreases canonical Wnt signaling in colon carcinoma cells and reduces tumor growth in conditional APC mutant mice. Cancer Res 2012;72:2822–32.
28. Semënov M, Tamai K, He X. SOST is a ligand for LRP5/LRP6 and a Wnt signaling inhibitor. J Biol Chem 2005;29:26770–5.
29. Oloumi A, Syam S, Dedhar S. Modulation of Wnt3a-mediated nuclear beta-catenin accumulation and activation by integrin-linked kinase in mammalian cells. Oncogene 2006;25:7747–57.
30. Kumar R, Balasenthil S, Pakala SB, Rayala SK, Sahin AA, Ohshiro K. Metastasis-associated protein 1 short form stimulates Wnt1 pathway in mammary epithelial and cancer cells. Cancer Res 2010;70:6598–608.
31. Nakashima N, Huang CL, Liu D, Ueno M, Yokomise H. Intratumoral Wnt1 expression affects *survivin* gene expression in non-small cell lung cancer. Int J Oncol 2010;37:687–94.
32. Verras M, Brown J, Li X, Nusse R, Sun Z. Wnt3a growth factor induces androgen receptor-mediated transcription and enhances cell growth in human prostate cancer cells. Cancer Res 2004;64:8860–6.
33. Katoh M. Regulation of Wnt3 and Wnt3A mRNAs in human cancer cell lines NT2, MCF-7, and MKN45. Int J Oncol 2002;2:373–7.
34. Harland R, Gerhart J. Formation and function of Spermann's organizer. Annu Rev Cell Dev Biol 1997;13:611–67.
35. Zhu Y, Parada LF. The molecular and genetic basis of neurological tumours. Nat Rev Cancer 2002;2:616–26.
36. Holland EC. Glioblastoma multiforme: the terminator. Proc Natl Acad Sci 2000;97:6242–4.
37. Cancer Genome Atlas Research Network. Comprehensive genomic characterization defines human glioblastoma genes and core pathways. Nature 2008;455:1061–8.
38. Zhang LY, Ye J, Zhang F, Li FF, Li H, Gu Y, et al. Axin induces cell death and reduces cell proliferation in astrocytoma by activating the p53 pathway. Int J Cancer 2009;35:25–32.
39. Kim MJ, Chia IV, Costantini F. SUMOylation target sites at the C terminus protect Axin from ubiquitination and confer protein stability. FASEB J 2008;22:3785–94.
40. Lui TT, Lacroix C, Ahmed SM, Goldenberg SJ, Leach CA, Daulat AM, et al. The Ubiquitin specific protease USP34 regulates Axin stability and Wnt/β-catenin signaling. Mol Cell Biol 2011;10:2053–65.
41. Kim S, Jho EH. The protein stability of Axin, a negative regulator of Wnt signaling, is regulated by Smad ubiquitination regulatory factor 2 (Smurf2). J Biol Chem 2010;285:36420–6.

Published OnlineFirst April 25, 2013; DOI: 10.1158/1535-7163.MCT-12-1176-T

Molecular Cancer Therapeutics

Identification and Characterization of a Small-Molecule Inhibitor of Wnt Signaling in Glioblastoma Cells

Alessandra De Robertis, Silvia Valensin, Marco Rossi, et al.

Mol Cancer Ther 2013;12:1180-1189. Published OnlineFirst April 25, 2013.